HEAT TRANSFER AND PRESSURE DROP DURING EVAPORATION AND CONDENSATION OF R134a INSIDE TWO MICROFIN TUBES OF NEW DESIGN

L. Colombo, A. Lucchini, A. Muzzio, A. Niro
Dipartimento di Energetica – Politecnico di Milano, Milan, Italy

Abstract

Saturated flow boiling and convective condensation experiments for oil-free Refrigerant-134a have been carried out with two microfin tubes with a new cross-section profile, as well as with a smooth one. All tubes have the same outer diameter of 9.52 mm; they are horizontally operated and are heated/cooled by a water stream. Both microfin tubes are characterized by sharp fins (apex angle of 40°) alternating with two different heights whereas the fin number is different, namely, 54 and 82, respectively. Evaporation tests are carried out at a nominal temperature of 5°C, for a mass flux ranging from about 100 to 340 kg/(m^2s), inlet quality between 0.25 and 0.70, and quality change varying from 0.10 to 0.70, whereas for the condensation tests the nominal temperature is 35°C, the mass flux varies between 100 and 440 kg/(m^2s), the inlet quality ranges from 0.75 to 0.10 and the quality change from 0.10 to 0.70. Finally, the paper presents comparisons between experimental data and estimates obtained by recent correlations specifically proposed for these tubes.

1. Introduction

Microfin tubes have outstanding performance in enhancing heat transfer for both evaporation and condensation and have been widely used in the air-conditioning and refrigeration industries. Thus, in recent years, many efforts have been spent in designing and developing microfin geometries which could provide high heat transfer coefficients and low pressure drop penalty.
Heat transfer characteristics of microfin tubes have been extensively studied over the past twenty years; detailed literature reviews are presented by Schlager (1991), Webb (1993), Webb (1994), Thome (1994), Kandlikar and Raykoff (1996). Several papers focused on the effects of various geometrical parameters such as tube diameter, spiral angle, fin height and shape, spacing between the fins and the number of fins [Yasuda et al. (1990), Eckels and Pate (1992), Oh and Bergles (1998)] and proposed predictive correlations for both heat transfer and pressure drops [Haraguchi et al. (1993), Kandlikar (1996), Wang and Kuo (1996), Kedzierski and Goncalves (1997), Nozu et al. (1998), Yu and Koyama (1998), Cavallini et al. (1998), Cavallini et al. (2000), Chamra et al. (2004), Chamra et al. (2005)]. However, due to the complexity of the physical phenomena involved in fluid-dynamics and heat transfer, experimental research is still the most reliable approach to the study of the performances of new microfin tubes and refrigerants.
Moved by these reasons, we are currently performing an experimental investigation of flow boiling and convective condensation of halo-carbon refrigerants inside microfin tubes as described in Muzzio et al. (1998). This paper reports on average heat transfer coefficient and pressure drop during evaporation and condensation of oil-free refrigerant R134a in a smooth tube and two microfin tubes with new cross-section profiles. The main difference between the microfin tubes consists in the number of fins so that, from the comparison of the performance, the effect of this parameter can be inferred. All the tubes have the same outer diameter of 9.52 mm and are horizontally operated.

2. Experimental Apparatus

The schematic diagram of the experimental facility is shown in Figure 1. The rig consists of three circuits, namely, a sealed refrigerant circuit, a water circuit to heat or cool the refrigerant in the test section, and a chilled coolant (water-glycol solution) circuit.

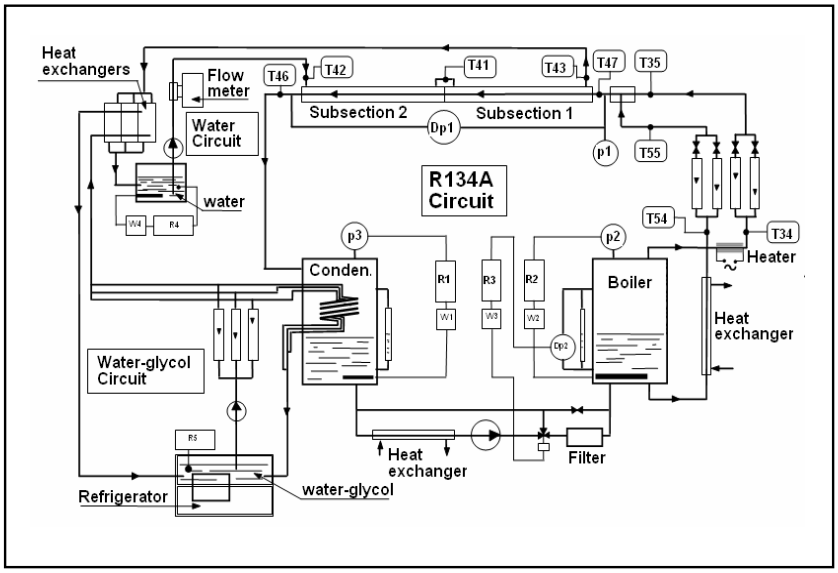

Figure 1. Schematic diagram of the experimental facility. Absolute and differential pressure transducers, temperature sensors, PID controllers and actuators are indicated respectively with p, Dp, T, R and W.

The main components of the refrigerant circuit are a boiler, the test section, a condenser, a gear pump and a filter dryer. The boiler is a 58 dm^3, stainless-steel pressure vessel of cylindrical shape with welded ellipsoidal heads; a heater, consisting of three electrical cartridges of 1, 1.5 and 2.5 kW power, is placed in the boiler bottom. Liquid and vapour are drawn from the boiler through two distinct lines. On each line the refrigerant mass flow rate is measured by means of Coriolis-type meters. A double-pipe subcooler is mounted on the liquid line upstream of the flow meters to ensure a single phase flow through them for any operating conditions. For the same reason, a ribbon electrical heater is wounded around the vapour line upstream of the flow meters. The liquid and vapour flow rates are controlled by precision metering valves. Downstream of the valves, vapour is mixed with liquid; the two-phase mixture flows through a 1.5 m long calming section and then enters the test section. At the exit, refrigerant flows through a second calming section (1.8 m) and then is discharged to the condenser, which maintains the test section outlet pressure at a given value. The condenser is a pressure vessel with the same shape and dimension as the boiler; three round coil heat exchangers are located inside the upper part of condenser; an electrical cartridge of 1 kW power is mounted in the condenser bottom. Finally, the liquid phase of the refrigerant is drawn from the condenser by a gear pump and is conveyed through a filter dryer to the boiler. Another double-pipe heat exchanger is mounted on the pump suction line to ensure a liquid flow through the pump. Refrigerant temperature is measured upstream of the flow meters, downstream of the controlling valves, and at the inlet and outlet of the test section by thermocouples inserted in 60 mm long, 3 mm o.d., stainless steel L-shaped wells located on the duct axis.

The test section is a straight, 2.6 m long, 9.52 mm o.d., copper tube that is divided in two identical parts, which we refer to as subsections. They are connected to each other and to the loop, without any change in the duct internal diameter, via three 3-way 12 mm tee fittings. Two pressure taps are drilled in each junction; the gap between the inner surface of the fitting and the outer surface of the tube serves as a pressure annular-chamber; pressure taps are connected via a manifold to pressure transducers. The refrigerant pressure is measured with a strain-gauge transducer (2 MPa full scale value), whereas pressure drop along the test section with an inductive differential pressure transducer (25 kPa full scale value, 1% o.f.s. accuracy). Both subsections are equipped with four T-type thermocouples to measure wall temperatures, which are placed in pairs at 140 mm from either ends; in each pair, thermocouples are 180 degrees apart. Thermocouple wires are 0.15 mm diameter, and they are cemented in longitudinal grooves (80 mm long, 0.5 mm large and 0.2 mm deep) cut in the outside wall of the tube.

Every subsection is enclosed by a 14 mm i.d. brass tube in order to create an annulus through which the heating or cooling water is circulated. Such a jacket is mounted on the subsection via two tee fittings which also allow the water to enter and leave the annulus. The distance between the inlet and discharge ducts of the jacket is 1.12 m; this distance is assumed as the active heat transfer length for the subsection. Calming and test sections are insulated by a 10 cm thick, glass-wool annulus, whereas a 2 cm thick, foam plastic sheets or annuli are used for the other circuit components and pipes.

Table 1. Geometrical parameters of the tested tubes.

Parameter	VA	HVA	smooth
Outside diameter [mm]	9.52	9.52	9.52
Maximum inside diameter [mm]	8.92	8.62	8.92
Bottom wall thickness [mm]	0.30	0.45	0.30
Higher fin height [mm]	0.23	0.20	-
Lower fin height [mm]	0.16	0.17	-
Apex angle	40°	40°	-
Number of grooves	54	82	-
Helix angle	18°	18°	-
Inside-surface area ratio	1.58	1.84	1

The water circuit consists of a tank provided with a heater, a centrifugal pump, the jackets surrounding the test section, a water-to-water heat exchanger. Demineralised water is drawn from a 30 dm^3, stainless steel tank equipped with a 5 kW power heater. Water flows inside the jackets surrounding the test section in counterflow with the refrigerant. Downstream the last jacket, water enters a plate heat exchanger in counter flow with the chilled coolant, and then it is discharged into the tank. The volume flow rate of water is measured by an inductive flow meter (0.15 dm^3/s full scale value). The bulk temperature of the water stream is measured by three thermal probes, located at the inlet of each subsection and at the outlet of the last one, respectively. Each probe consists of three T-type thermocouples cemented in three fine wells drilled in a copper cylinder with an outer diameter of 13 mm and a height of 20 mm. Such a cylinder reduces the area of stream cross-section, thus promoting flow mixing and hence equalisation of the liquid temperature. Furthermore, since thermocouples are connected in series, the measured voltage is proportional to the sum of temperatures taken in three different points of the cylinder; we assumed the temperature corresponding to one third of the voltage as representative of the cylinder mean temperature. A 100 Ω Pt-resistor is employed to measure the water temperature in the tank.

Finally, the chilled coolant circuit is filled with a water-glycol solution and it consists of a commercial refrigeration unit and a centrifugal pump. Such a circuit provides the cold medium circulated in the heat exchangers placed in the refrigerant condenser or mounted on both the refrigerant and the water circuits.

The microfin tubes tested are Metofin 952-30VA40/54A and 952-45HVA40/82 manufactured by Trefimetaux. They have the same outer diameter of 9.52 mm and for sake of simplicity we will denote them as VA- and HVA-tube respectively. The main feature distinguishing them from other microfin tubes of new design is that fins alternate with two different heights. Between each other they differ essentially in the fin number as shown in Table 1, where the main geometrical parameters are listed together with those of the smooth tube. This table also reports the heat transfer internal surface ratio with respect to the smooth tube.

3. Test procedures and data reduction

Signals from thermocouples and transducers are cyclically read by a data acquisition unit HP3497 and sent to an on-line PC. In order for all variables to be affected by similar RMS relative errors, the measurements of refrigerant temperature, pressure drop, refrigerant mass flow rate and water flow rate are based on 30, 50, 50 and 100 readings for cycle, respectively. Every experimental datum, instead, is obtained by averaging the measurements of ten cycles in order to reduce the influence of random errors and fluctuations. Finally, for every operating condition, more than ten experimental data are collected. The heat transfer coefficient is computed as follows. We assume that the refrigerant temperature varies linearly between the value T_{in}, measured at the entrance of the test section, and the value T_{out} computed at the exit as $T_s(p_s(T_{in})-\Delta p)$, where T_s is the function correlating the saturation temperature to the pressure, p_s the inverse function of T_s, and Δp the pressure drop measured along the test section. Then, for each subsection we calculate the mean refrigerant temperature $T_{r.m,i}$, the mean wall temperature $T_{w.m,i}$, the refrigerant to wall temperature mean difference $\Delta T_{m,i} = (T_{w.m,i}-T_{r.m,i})$, and the heat transfer coefficient $h_i=q_i/\Delta T_{m,i}$ where q_i is the mean heat flux based on a nominal inside area corresponding to the maximum internal diameter, i.e. the diameter at the root of microfins. Eventually, we compute the average heat transfer coefficient

for the test section as the arithmetic mean of the subsection coefficients h_i. Relevant variables for the present investigation are affected by the following representative experimental uncertainties measured or estimated by a propagation error analysis: ±0.35% for the refrigerant mass flow rate, ±1.3% for the inlet quality, ±0.2 K between the refrigerant temperature and the saturation one, ±0.03 K between the wall and refrigerant temperatures with the refrigerant trapped in the test section and the water flowing, ±1.0% for the refrigerant pressure drop, ±1.0% for the water volume flow rate, ±0.02 K for the water temperature difference between the subsection inlet and outlet, ±1.4% for the heat rate, and ±7% for the average heat transfer coefficient, by assuming a temperature difference between wall and refrigerant equal to 2 K.
Properties of R134a were determined with reference to JAR Tables (1990).

4. Results and discussion

In saturated flow boiling or convective condensation, for fixed test section configuration, i.e., dimension and shape of the cross section, length, orientation with respect to gravity, both pressure drop and average heat transfer coefficient depend on four independent variables, namely, total mass flow rate, temperature (or pressure), inlet thermodynamic quality and heat rate. Since the quality change along the test section depends linearly on heat rate, a different but equivalent parameterisation can be obtained by substituting the former with the latter quantity in the list of the independent variables. Experimental tests were carried out at fixed saturation temperature, varying in turn the mass flow rate, the inlet quality and the quality variation, in order to assess clearly the influence of each variable on both heat transfer and pressure drop.
Evaporation tests are carried out at a nominal temperature of 5°C (±0.2 K) corresponding to a pressure of 0.350 MPa, for a mass flux ranging from about 100 to 340 kg/(m^2s), inlet quality between 0.25 and 0.70, and quality change varying from 0.10 to 0.70, whereas for the condensation tests the nominal temperature is 35 °C (±0.2 K) corresponding to a pressure of 0.887 MPa, the mass flux varies between 100 and 440 kg/(m^2s), the inlet quality ranges from 0.75 to 0.10 and the quality change from 0.10 to 0.70.
In the following subsections experimental data on evaporation and condensation are presented and discussed, respectively. It is to be noted that pressure drops per unit length are referred to the full length of the test section that is 2.6 m, while Nusselt numbers are computed on the basis of the maximum inside diameter of the tube.

4.1. Experimental data on evaporation

Because of time constraints, evaporation tests were performed only on the HVA tube. Figure 2 shows the boiling heat transfer coefficient h_b plotted versus the mass flux G for the tested microfin

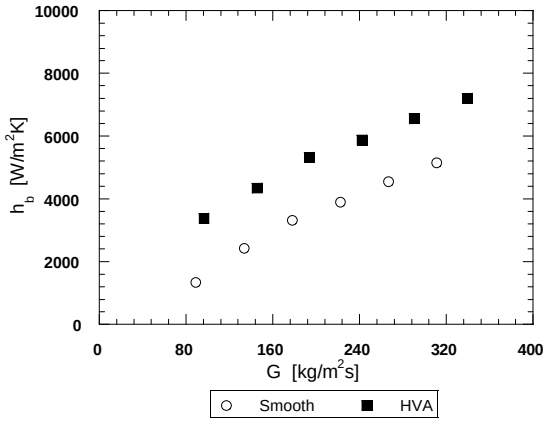

Figure 2. Flow-boiling heat transfer coefficient h_b versus mass flux G for fixed inlet quality x_{in}=0.30 and quality change Δx=0.30.

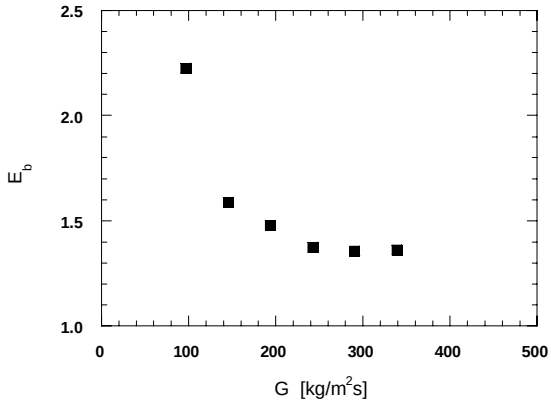

Figure 3. Enhancement factor E_b versus mass flux G for fixed inlet quality x_{in}=0.30 and quality change Δx=0.30.

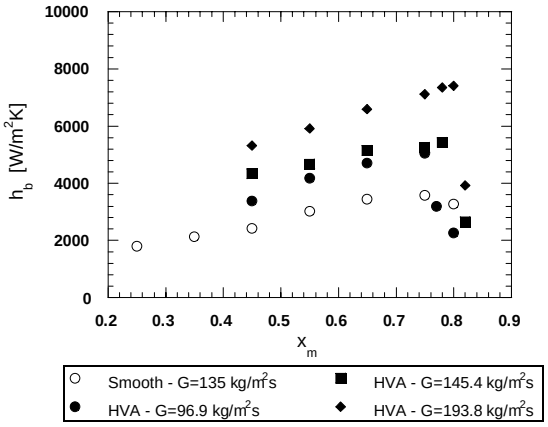

Figure 4. Flow-boiling heat transfer coefficient h_b versus average quality x_m for fixed mass flux G and quality change Δx=0.30.

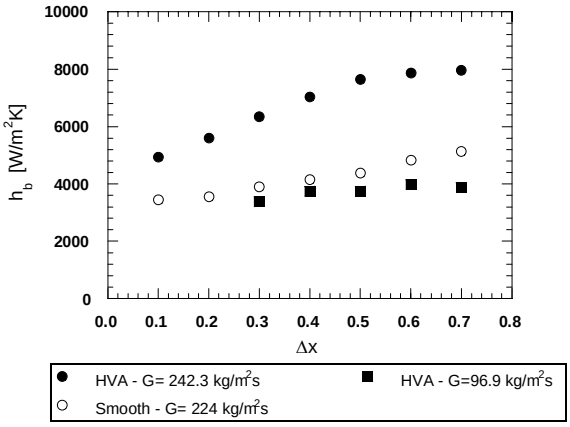

Figure 5. Flow-boiling heat transfer coefficient h_b versus quality change Δx for fixed mass flux G and average quality x_m=0.45.

tube HVA; data obtained on the smooth tube are also included for comparison. For such data, nominal inlet quality and quality change are x_{in}=0.30 and Δx=0.30, respectively. In considering this figure it is worth keeping in mind that as the mass flux increases at constant Δx a corresponding variation in heat flux sets up. For the data here reported, the average heat flux ranges between 5.1 and 17.8 kW/m^2.

As expected, the boiling heat transfer coefficient is an increasing function of G and the rate of increase is higher for lower values of the mass flux. This behaviour could be explained in considering that at low mass fluxes saturated boiling largely contributes to the heat transfer and in boiling the heat transfer coefficient grows rapidly with heat flux; increasing G, convective evaporation sets up and the growth of the heat transfer coefficient is essentially linked to that of the mass flux. Of course heat transfer for the microfin tube results higher than that for the smooth tube. Differences in thermal performances are well accounted by the enhancement factor E_b, defined as the ratio of the heat transfer coefficient of the microfin tube to that of the smooth tube, depicted in Figure 3. It is a decreasing function of the mass flux: fins are probably more effective at low values of the mass flux because they act both as turbulence promoters and as providing numerous nucleation sites. Increasing G, E_b seems to tend asymptotically to about 1.4, that is, a value smaller than the internal surface ratio. This result does not conform to the remark by Eckels and Pate (1992) who, on the basis of the findings of their experimental studies, concluded that at high mass flux, the heat transfer increase in the microfin tube is due to the area increase. On the contrary, even at high mass flux, our data support the observation by Ito and Kimura (1979) that the increase in boiling heat transfer coefficient cannot be explained simply on the basis of area extension.

The effect of average quality x_m on the evaporation heat transfer coefficient, for fixed mass flux and quality change (Δx=0.30), is shown in Figure 4. For the microfin tube, a distinct maximum in heat transfer coefficient is observed at high average vapour quality, ranging from about 0.75 to 0.80. The

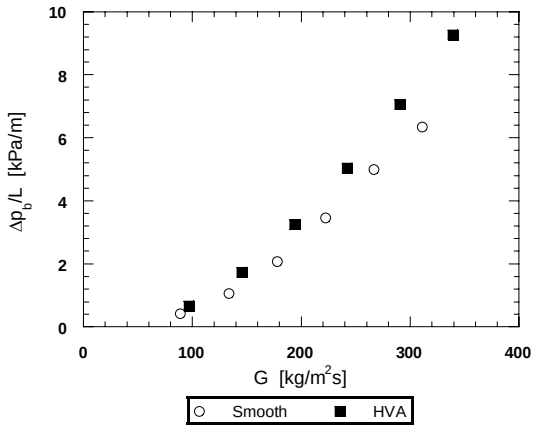

Figure 6. Flow-boiling pressure drop $\Delta p_b/L$ versus mass flux G for fixed inlet quality x_{in}=0.30 and quality change Δx=0.30.

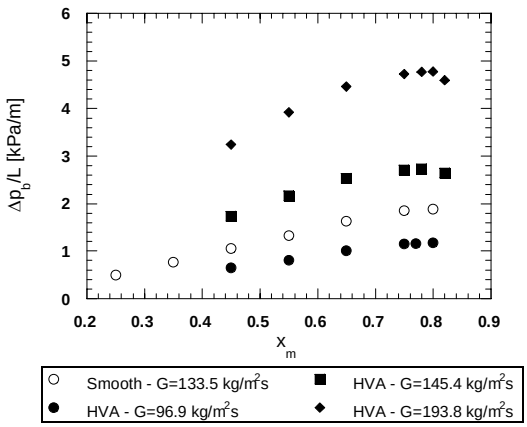

Figure 7. Flow-boiling pressure drop $\Delta p_b/L$ versus average quality x_m for fixed mass flux G and quality change Δx=0.30.

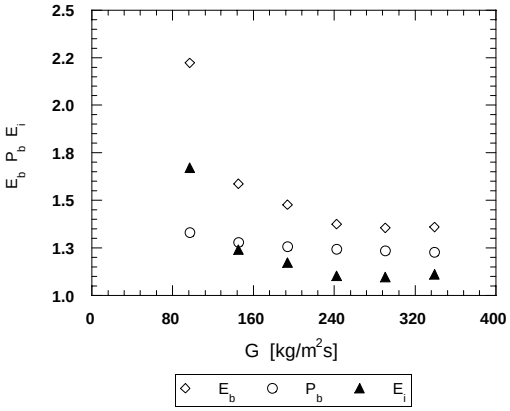

Figure 8. Enhancement factor E_b, penalty factor P_b, and efficiency index E_i versus mass flux for x_{in}=0.30 and Δx=0.30.

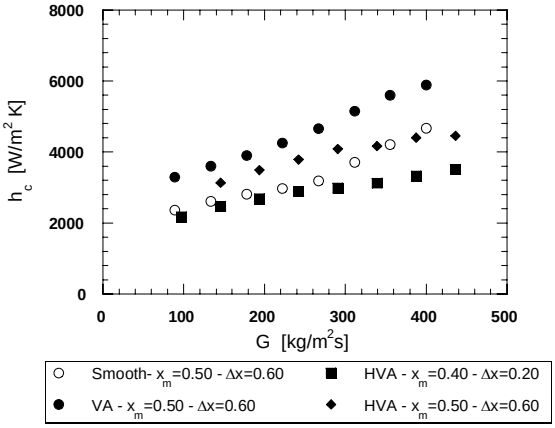

Figure 9. Condensation heat transfer coefficient h_c versus mass flux G for fixed average quality x_m and quality change Δx.

corresponding value of x_m seems to increase slightly with the mass flux. The fall off in the heat transfer coefficient after the peak is caused by the dryout onset. In fact, heat transfer data relevant to the second subsection, not reported here, indicate that dryout occurs at a vapour quality of approximately 0.9. For the smooth tube, instead, a slightly marked maximum, located approximately at x_m=0.7, is observed. The comparison between the data for the HVA tube at G=145.4 kg/(m^{2}s) and those for the smooth one at about the same mass flux shows that microfinning seems to provide, in addition to the substantial heat transfer enhancement, a shift of the dryout occurrence in the region of higher qualities. This might be due to the effect of both capillarity and centrifugal force that cause the wall to be kept wet longer. Moreover, the heat transfer augmentation decreases with increasing vapour quality.

The influence of the quality change (heat flux) for given mass flux and average quality x_m=0.45 is depicted in Figure 5. We see that the heat transfer coefficient is not strongly affected by the quality change at G=96.9 kg/(m^{2}s). However, for G=242.3 kg/(m^{2}s) it may be noted that h_b is an increasing function of quality variation, up to $\Delta x \cong 0.50$; then the rise lowers and the trend seems to flatten. Instead the smooth channel at about the same mass flux exhibits a weak increase of the heat transfer coefficient with quality variation.

Attention will now be focused on pressure drop. Figures 6 and 7 display data for the evaporation pressure drop, obtained in the same conditions reported in Figures 2 and 4, respectively. For all the tubes, pressure drop increases significantly with mass flux and quality. However, at higher vapour quality pressure drop falls off toward the data point for the only vapour phase pressure drop. The influence of quality change appears to be negligible. As expected, the microfin tube displays pressure drops higher than those of the smooth tube. This can be evidenced defining a penalization factor P_b, as the ratio of the pressure drop in the microfin tube to that in the smooth tube. Moreover, an efficiency index of the microfin tube can be defined as $E_i = E_b/P_b$. In Figure 8 the enhancement factor, the penalization factor and the efficiency index, obtained by interpolation of the data, are reported as functions of the mass flux, for x_m=0.45 and Δx = 0.30. It can be noticed that the efficiency index, starting from a value of 1.67, seems to tend asymptotically to 1.1; it is, thus, slightly greater than unity. Representative values of sample variances for measurements of heat transfer coefficients and pressure drops in the microfin tube are reported in Table 2.

Table 2. Example of statistical analysis of data.

x_m=0.30 - Δx=0.30				
G [kg/(m^{2}s)]	$\mathbf{h_b}$ (mean) [W/(m^{2}K)]	$\boldsymbol{\sigma_h}$ (std. dev.) [W/(m^{2}K)]	**Δp/L** (mean) [kPa/m]	$\boldsymbol{\sigma_p}$ (std. dev.) [kPa/m]
96.9	3378.5	24.4	0.660	0.008
145.4	4344.5	37.6	1.733	0.016
193.8	5321.3	53.7	3.242	0.022
242.3	5879.3	37.6	5.036	0.024
290.7	6544.5	20.0	7.056	0.021
339.2	7195.3	31.3	9.270	0.039

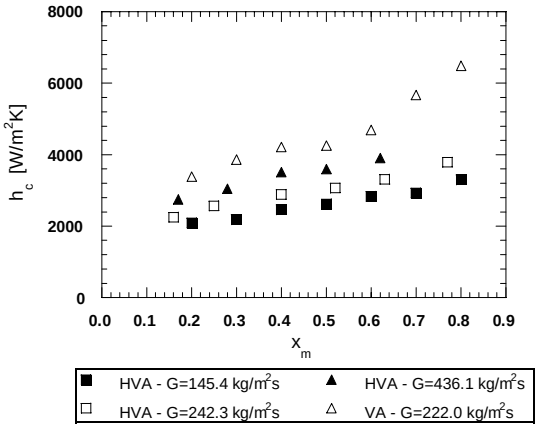

Figure 10. Condensation heat transfer coefficient h_c versus average quality x_m for fixed mass flux G and quality change Δx=0.20.

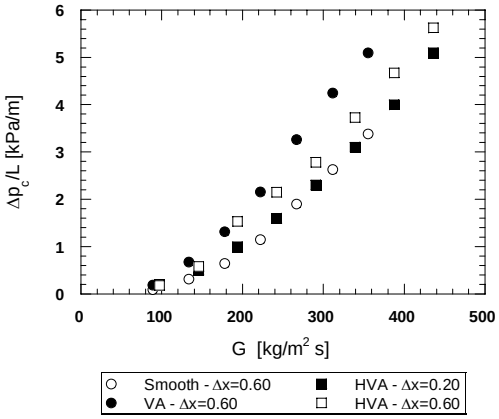

Figure 11. Condensation pressure drop $\Delta p_c/L$ versus mass flux G for fixed average quality x_m=0.40 and quality change Δx.

4.2. Experimental data on condensation

Figure 9 displays the average heat transfer coefficient h_c plotted versus the mass flux G for the microfin and smooth tubes. As already observed, a mass flux variation at constant Δx is accompanied by a variation in heat flux; for the data here reported, the average heat flux ranges from 1.5 to 13.2 kW/m^2. As expected, the heat transfer coefficient is an increasing function of G, but the trend for the microfin tubes differs from that of the smooth tube. For the latter, data exhibit a linear-at-interval dependence on G with a change of slope approximately at G=250 kg/(m^{2}s). Supported by visual observations, we infer that in the first region, where heat transfer is weakly dependent on the mass flux, the flow is stratified, whereas it is annular when h_c starts to increase more steeply with G. Both the microfin tubes exhibit in the same conditions higher values of the heat transfer coefficient and data do not display any change of slope marking the transition from stratified to annular flow. However, it may be noted that the trend for the HVA-tube, in contrast with the VA-tube, flattens for high values of the mass flux and tends to the corresponding values of the smooth tube. Differences in thermal performances can be appreciated by considering the enhancement factor E_c. For both tubes the enhancement factor remains lower than the inside-surface area ratio. In fact, for the VA-tube the enhancement factor varies within 1.25 and 1.5 whereas for the HVA tube it ranges from 1 and 1.38. These values clearly show the better performance of the VA geometry with respect to the HVA geometry, from the thermal standpoint. Since the VA and HVA tubes have quite similar geometries which essentially differ only in the fin number, we infer that a large number of fins decreases the enhancement in condensation, in accordance with the findings of Yasuda et al. (1990).

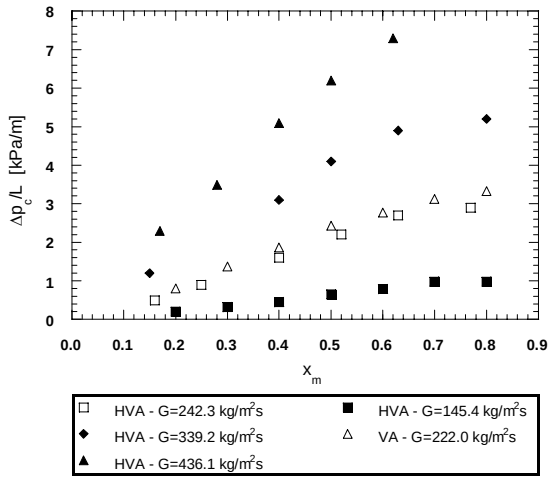

Figure 12. Condensation pressure drop $\Delta p_c/L$ versus average quality x_m for fixed mass flux G and quality change Δx=0.20.

Figure 10 depicts the effect of the average quality on the condensation heat transfer coefficient. It is seen that h_c increases with quality at constant mass flux and quality change. In particular, when comparing the two microfin tubes at almost equal mass flux (242.3 and 222 kg/(m^{2}s)) and with Δx=0.2, it is seen that the rate of increase is much higher for the VA tube than for the HVA tube, confirming the above consideration; moreover the HVA tube exhibits a behaviour quite similar to that, not shown, of the smooth tube.

As for the influence of the quality change, data (not reported here) show that the heat transfer coefficient increases with increasing Δx.

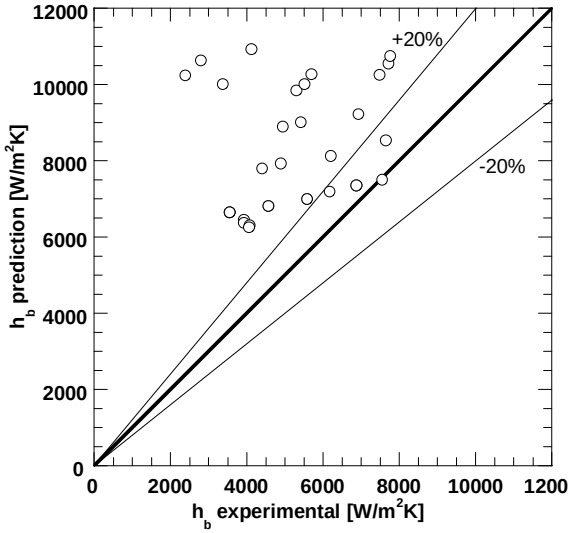

Figure 13. Comparison between experimental data and predictions of the Cavallini et al. correlation for the heat transfer coefficient.

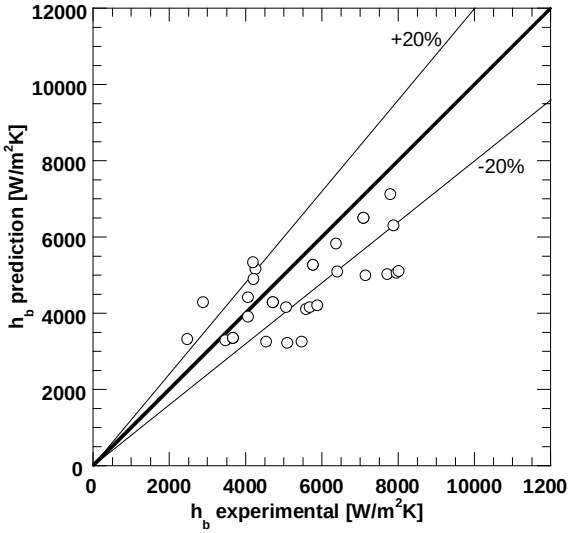

Figure 14. Comparison between experimental data and predictions of the Kandlikar scheme of correlation for the heat transfer coefficient.

However, only moderate variations of heat transfer are displayed in the range of the tested quality change.

Condensation pressure drop for x_{in}=0.50 and x_{out}=0.30 is plotted versus mass flux and average quality in Figures 11 and 12 respectively. As for boiling, pressure drop is an increasing function of G and for both microfin tubes it is greater than that of the smooth tube. Moreover the values are quite similar. With reference to the effects of average quality, the experimental data show that at fixed mass flux and quality change (222 and 242.3 kg/(m^{2}s); Δx=0.20) pressure drop increases with average quality varying over the range between 0.20 and 0.80. Penalty factors P_c, which are in fact the same for both microfin tubes, range from 2 to 1.4. For the presented data, values of sample variances for measurements of heat transfer coefficients and pressure drops in the microfin tube are comparable to those reported for evaporation in Table 2.

5. Comparison with correlations

Several correlations for both condensation and evaporation of refrigerants inside enhanced tubes were selected from the literature to carry out comparisons with the presented data. It should be noted that all the correlations considered predict local values of the quantities of interest. Therefore, the local distributions of both heat transfer coefficient and pressure drop were calculated, supposing a linear variation of the quality between the inlet and the outlet of the tube. Then, the average values over the tube length were determined. Moreover, since, as already noticed, fins in the tube alternate with two different heights, a mean fin height of 0.185 mm were used, if a fin height specification was required. In the next two subsections comparisons between experimental data and predictions for evaporation and condensation are reported, respectively.

5.1. Correlations for evaporation

As already observed experimental data are now available only for the HVA tube. The Cavallini et al. (1998) correlation and the Kandlikar (1996) scheme of correlation were considered for the heat transfer coefficient and data for pressure drop were compared with predictions of the Wang and Kuo (1996) correlation.

Results for the heat transfer coefficient are reported in Figures 13 and 14. In considering the Cavallini et al. correlation (Figure 12) it was observed that it overpredicts the data particularly at the lower values of the mass flux; actually, the mean deviation is 74.5% and the standard deviation is 74.0%.

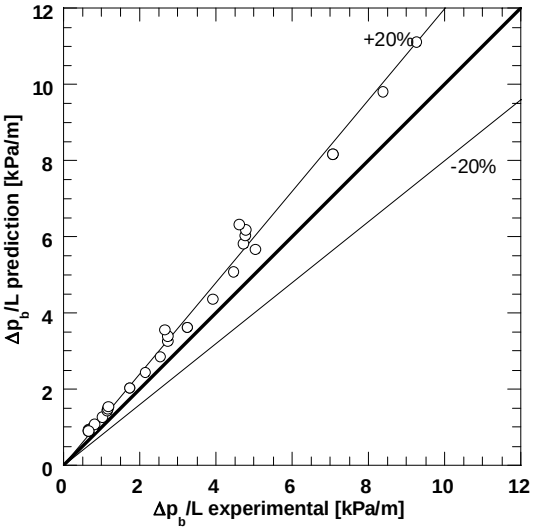

Figure 15. Comparison between experimental data and predictions of the Wang and Kuo correlation for pressure drops.

Using the Kandlikar scheme of correlation (Figure 14), the parameters n, E'_{cb} and E'_{nb} were determined, as suggested by the author, by a minimization of the mean squared error between prediction and data; thus the corresponding values resulted 0.6, 0.3019 and 0.1286. In this case the agreement with the experimental data is good for variable mass flux and quality variation. It is worth noting that the correlation gives a heat transfer coefficient essentially constant with the average quality in the investigated range and the model is unable to predict the dryout onset. The mean deviation and the standard deviation are respectively E=9.9% and σ=21.8%.

Regarding the pressure drop, in the application of the Wang and Kuo correlation the parameter f_{tp} was considered independent of the Reynolds number and set to 0.0139 as suggested by the authors for microfin tubes. The agreement with the experimental data (Figure 15) is satisfactory for all the operating conditions: the mean deviation is 24.4% and the standard deviation is 9.5%.

5.2. Correlations for condensation

The correlations of Cavallini et al. (2000), Yu and Koyama (1998) and Kedzierski and Goncalves (1997) were selected for the heat transfer coefficient, whereas the correlations of Cavallini et al. (2000), Kedzierski and Goncalves (1997), Haraguchi et al. (1993) and Nozu et al. (1998) were considered for the pressure drop. Attention will be devoted first to the heat transfer coefficient for the VA tube. As it can be seen from Figures 16, 17, 18, the predictions of the Cavallini et al. correlation agree very well with the data and turns out to be more correct in trend than the correlations of Kedzierski and Goncalves and Yu and Koyama. With the Cavallini et al. correlation (Figure 16), all of the data are predicted within ±20%, with a mean deviation E=3.4% and a standard deviation σ=6.5%. The most significant deviations occur at high mass flux, where the correlation tends to underpredict the experimental data. The mean deviation and the standard deviation of the Kedzierski and Goncalves correlation (Figure 17) are 13.5% and 15%, respectively. This correlation tends to overpredict the experimental data, particularly at high average vapour

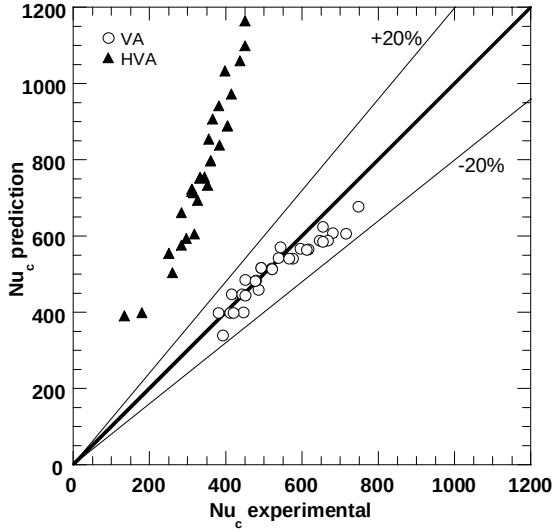

Figure 16. Comparison between experimental data and predictions of the Cavallini et al. correlation for the average Nusselt number.

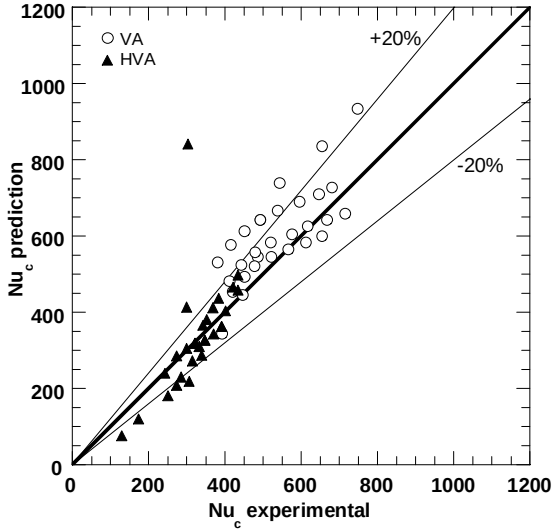

Figure 17. Comparison between experimental data and predictions of the Kedzierski and Goncalves correlation for the average Nusselt number.

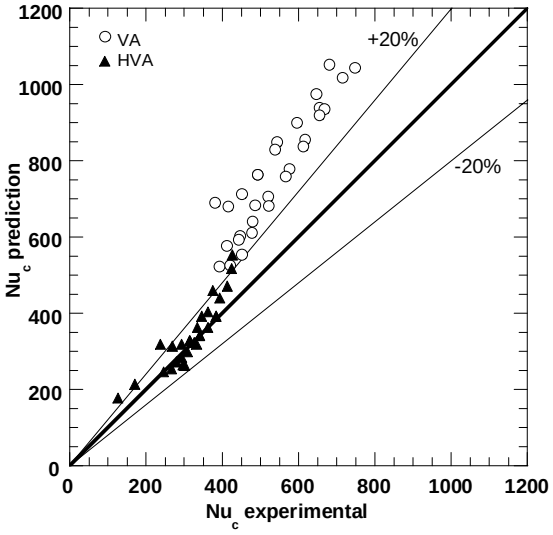

Figure 18. Comparison between experimental data and predictions of the Yu and Koyama correlation for the average Nusselt number.

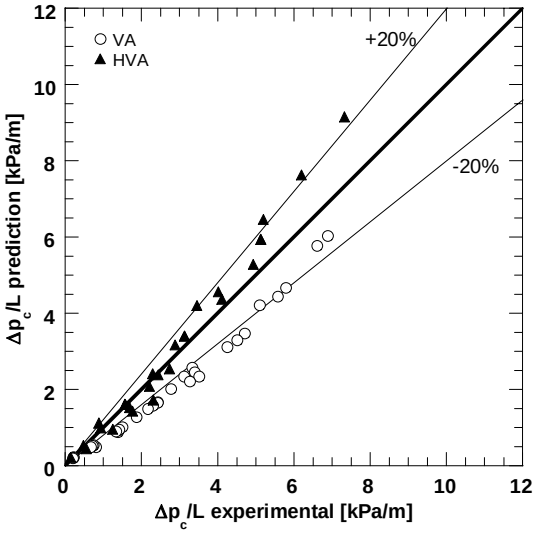

Figure 19. Comparison between experimental data and predictions of the Haraguchi et al. correlation for pressure drops.

quality and at low mass fluxes.

The Yu and Koyama correlation (Figure 18) is the worst predictor of the data with a mean deviation E=43.3% and a standard deviation σ=12.8%. This correlation consistently overpredicts all of the data with a deviation that exceeds 50% in some cases.

For the HVA tube the situation is reversed. The comparison among Figures 16, 17, 18 reveals that the Cavallini et al. correlation is the worst predictor, heavily overpredicting all the data, with a mean deviation E=127.8% and a standard deviation σ=20.9%. This behaviour could be related to the dependence of the correlation on the fin number, which is the main feature distinguishing the two microfin tubes. The Kedzierski and Goncalves correlation (Figure 17) leads to a good estimate of the data obtained varying the mass flux, slightly underpredictig at the higher values. Data are underpredicted at low values of the average quality, whereas they are overpredicted at higher values. Instead, the influence of the quality variation is highly overpredicted. In summary, the correlation exhibits a mean deviation E=1.49% and a standard deviation σ=36.9%.

From inspection of Figure 18, the Yu and Koyama correlation seems to be, in this case, the best predictor. All the data are correlated with a mean deviation E=7.7% and a standard deviation σ=12.9%. It was ovserved that the data are overpredicted at low values of the mass flux, but the agreement is strongly improved as the mass flux increases. The correlation overpredicts the data at variable average quality, giving the best results for intermediate values.

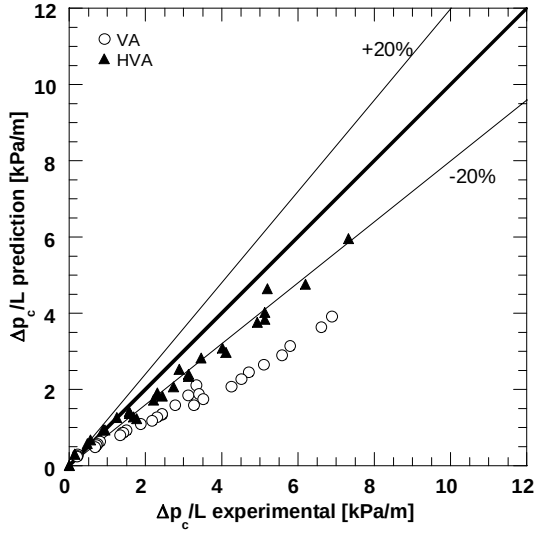

Figure 20. Comparison between experimental data and predictions of the Cavallini et al. correlation for pressure drops.

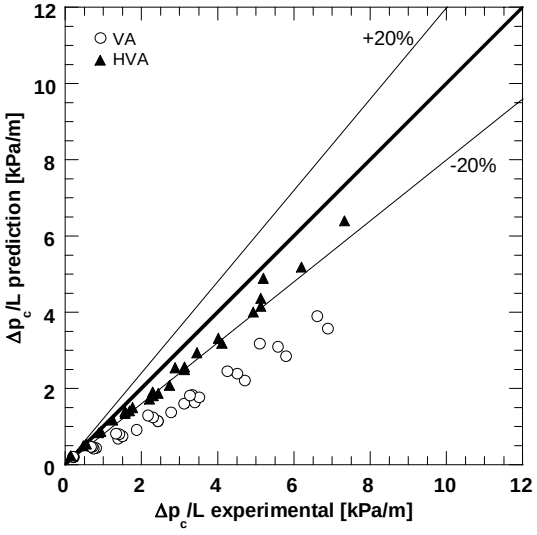

Figure 21. Comparison between experimental data and predictions of the Kedzierski and Goncalves correlation for pressure drops.

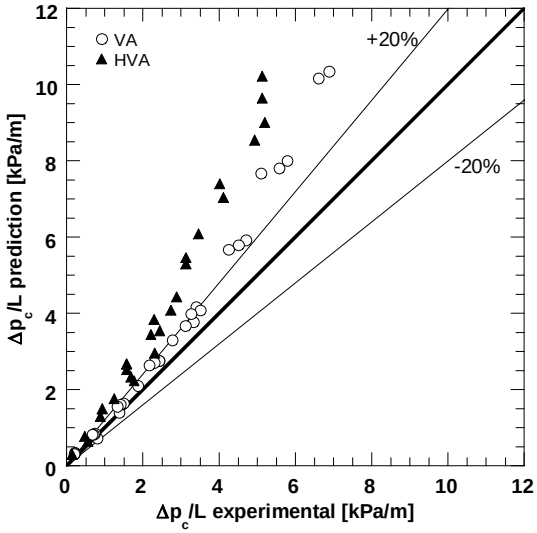

Figure 22. Comparison between experimental data and predictions of the Nozu et al. correlation for pressure drops.

Attention will now be turned to pressure drop, starting from the VA tube. The Haraguchi et al. correlation (Figure 19) proves to be the best predictor with a mean deviation of –24.0% and a standard deviation of 11.4 %, though it tends to underpredict the experimental data. The same tendency is exhibited also by the correlations of Cavallini et al. (E=–33.9% and σ=23.1%) and of Kedzierski and Goncalves (E=–40.5% and σ=15.8%), respectively shown in Figures 20 and 21. On the contrary, the Nozu et al. correlation (Figure 22) overpredicts the data with a mean deviation of 26.0% with σ=17.5%; despite this rather high deviation, the predictions of the correlation prove to be correct in trend. For the HVA tube, the Cavallini et al. and the Kedzierski and Goncalves correlations (Figures 20 and 21) show a similar behaviour, generally underpredicting the data. The former presents a mean deviation E=–11.2% and a standard deviation σ=23.0%. The latter exhibits essentially a lower standard deviation (E=–11.9% and σ=14.1%); its main difference from the other correlations is that it predicts a pressure drop slightly increasing with the quality variation. This behaviour is consistent with experimental data, even though it is always underpredicted. The agreement provided by the Haraguchy correlation (Figure 19) seems to be the best, in particular for the data collected at variable mass flux. However it was noticed that, increasing the average quality at fixed mass flux, data tends to be overpredicted and the agreement get worse for higher values of the mass flux. The mean deviation is 5.9% and the standard deviation is 16.2%. The Nozu et al. correlation (Figure 22) is the worst predictor of the data with deviations always greater than 30%. The mean deviation is 64.0% and the standard deviation is 22.1%.

6. Conclusions

It is well known that the microfin tube exhibits a significant heat transfer enhancement both in evaporation and condensation, when compared to the smooth tube. Generally, pressure drop also increases but less than heat transfer. However, the extent of heat transfer increase and pressure drop penalization is greatly dependent upon geometry. More specifically, regarding the present study, the following considerations may be pointed out. In boiling it was observed that microfins cause the dryout onset to be shifted towards higher values of vapour quality, in comparison with the smooth tube. This may be due to the combined action of capillarity and centrifugal force in keeping the wall wet longer (liquid is conveyed upward). In condensation, the comparison between the VA- and HVA-tube shows that the former has better performances than the latter: since they have very similar geometry and the main difference is in the number of fins (54 for the VA-tube, 82 for the HVA-tube) it may be inferred that a large number of fins could depress the mechanisms of heat transfer increase. Comparison between the predictions of various correlations from literature and experimental data both on heat transfer and pressure drop was proposed. In boiling, the best results for the heat transfer are given by the Kandlikar scheme of correlation, which presents a mean error of 9.9 % and a standard deviation of 21.8%, whereas, for the pressure drop, the Wang and Kuo correlation was used, giving a mean error of 24.4% and a standard deviation of 9.5%. In condensation however, where two different microfin tubes were considered, no definitive conclusions can be drawn: in fact, frequently, the correlation that gives the best agreement with data for a tube, does not work so well for the other one. Thus it could be inferred that the influence of geometry is still not completely described in the models considered.

Acknowledgements

This work is supported by MURST (the Italian Department for the University and for the Scientific and Technical Research) via COFIN 2004 grants.

References

Cavallini A., Del Col B., Doretti L., Longo G. A., Rossetto L., 1998, A new model for refrigerant vaporisation inside enhanced tubes, 3rd International Conference on Multiphase Flow, ICMF '98, Lyon, France.

Cavallini A., Del Col D., Doretti L., Longo G. A., Rossetto L., 2000, Heat Transfer and Pressure Drop During Condensation of Refrigerants Inside Horizontal Enhanced Tubes, Int. J. of Refrigeration, 23, 4-25.

Chamra L. M., Tan M., Kung C., 2004, Evaluation of existing condensation heat transfer models in horizontal micro-fin tubes, Experimental Thermal and Fluid Science, 28, 617-628, Elsevier.

Chamra L. M. et al., 2005, Modeling of condensation heat transfer of pure refrigerants in micro-fin tubes, International Journal of Heat and Mass Transfer, 48, 1293-1302.

Eckels S. J. and Pate M.B., 1992, Evaporation heat transfer coefficients for R-22 in micro-fin tubes of different configurations, HTD 202, 117-125.

Haraguchi H., Koyama S., Esaki J., Fujii T., 1993, Condensation Heat Transfer of Refrigerants HFC134a, HCFC123 and HCFC22 in a Horizontal Smooth Tube and a Horizontal Microfin Tube, Proc. 30th Symposium of Japan, Yokohama, 343-345.

Ito M. and Kimura H. 1979, Boiling heat transfer and pressure drop in internal spiral-grooved tubes, Bulletin of JSME, 2, 171, 1251-1257.

JAR, Japanese Association of Refrigeration, 1991, Thermophysical Properties of environmentally acceptable fluocarbons – HFC-134a and HCFC-123.

Kandlikar S. G. and Raykoff T., 1996, Predicting flow boiling heat transfer for refrigerants in microfin tubes, Proc. of 2nd European Thermal-Sciences and 14th UIT National Heat Transfer Conf., 1, 475-482.

Kedzierski M. A., Goncalves J. M., 1997, Horizontal Condensation of Alternative Refrigerants Within a Micro-Fin Tube, NISTIR 6095, US Departement of Commerce.

Muzzio A., Niro A. and Arosio S., 1998, Heat transfer and pressure drop during evaporation and condensation of R22 inside 9.52 mm O.D. microfin tubes of different geometries, Enhanced Heat Transfer, 5, 39-52.

Nozu S., Katayama H., Nakata H., Honda H., 1998, Condensation of a Refrigerant CFC11 in Horizontal Microfin Tubes (proposal of a correlation equation for frictional pressure gradient), Experimental Thermal and Fluid Science, 18, 82-96.

Oh S.Y., Bergles A.E., 1998, Experimental Study of the Effects of the Spiral Angle on Evaporative Heat Transfer Enhancement in Microfin Tubes, ASHRAE Transactions, 104, 2, 1137-1143.

Schlager L. M., 1991, Boiling and condensation in microfin tubes, VKI Lecture Series on Industrial Heat Exchangers.

Thome J. R., 1994, Two-phase heat transfer of new refrigerants, Heat transfer 1994, Proc. 10th Int'l Heat Transfer Conference, 1, 19-41.

Yasuda K., Ohizumi K., Hori M. and Kawamata O., 1990, Development of condensing thermofin-HEX-C tube, Hi-tachi Cable Rev., 9, 27-30.

Yu J., Koyama S., 1998, Condensation Heat Transfer of Pure Refrigerants in Microfin Tubes, Proceedings of the 1998 IRC Purdue, 325-330.

Wang C. C., Kuo C. S., 1996, In-tube evaporation of HCFC-22 in a 9.52 mm micro-fin / smooth tube, Int. Journal of Heat and Mass Transfer, 39, 2559-2569.

Webb R. L., 1993, Principles of enhanced heat transfer, 446-450, John Wiley & Sons, New York.

Webb R. L., 1994, Advances in modeling enhanced heat transfer surface, Heat transfer 1994, Proc. 10th Int'l Heat Transfer Conference, 1, 445-459.